Formation Mechanism and Optical Properties of InAs Quantum Dots on the Surface of GaAs Nanowires

ARTICLE *in* NANO LETTERS · MARCH 2012

Impact Factor: 13.59 · DOI: 10.1021/nl204204f · Source: PubMed

8 AUTHORS, INCLUDING:

Xin Yan
Beijing University of Posts and Telecommunic…
44 PUBLICATIONS **82** CITATIONS
SEE PROFILE

Xia Zhang
Shandong Cancer Hospital (Shandong Provinc…
243 PUBLICATIONS **2,111** CITATIONS
SEE PROFILE

Qi Wang
Beijing University of Posts and Telecommunic…
135 PUBLICATIONS **412** CITATIONS
SEE PROFILE

Yongqing Huang
Beijing University of Posts and Telecommunic…
255 PUBLICATIONS **657** CITATIONS
SEE PROFILE

NANO LETTERS

Letter

pubs.acs.org/NanoLett

Formation Mechanism and Optical Properties of InAs Quantum Dots on the Surface of GaAs Nanowires

Xin Yan, Xia Zhang,* Xiaomin Ren,* Xiaolong Lv, Junshuai Li, Qi Wang, Shiwei Cai, and Yongqing Huang

State Key Laboratory of Information Photonics and Optical Communications, Beijing University of Posts and Telecommunications, Beijing 100876, China

ABSTRACT: Formation mechanism and optical properties of InAs quantum dots (QDs) on the surface of GaAs nanowires (NWs) were investigated. This NW-QDs hybrid structure was fabricated by Au-catalyzed metal organic chemical vapor deposition. We found that the formation and distribution of QDs were strongly influenced by the deposition time of InAs as well as the diameter of GaAs NWs. A model based on the adatom diffusion mechanism was proposed to describe the evolution process of the QDs. Photoluminescence emission from the InAs QDs with a peak wavelength of 940 nm was observed at room temperature. The structure also exhibits a decoupling feature that QDs act as gain medium, while NW acts as Fabry–Perot cavity. This hybrid structure could serve as an important element in high-performance NW-based optoelectronic devices, such as near-infrared lasers, optical detectors, and solar cells.

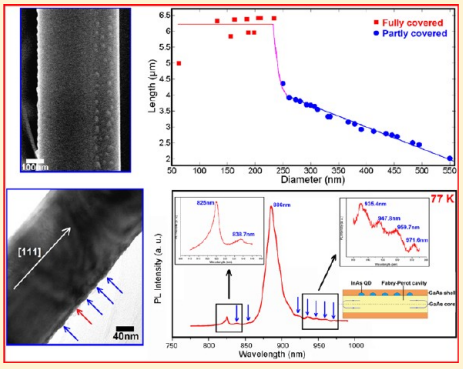

KEYWORDS: *Nanowire, quantum dots, MOCVD, formation mechanism, optical properties*

As two outstanding representatives of low-dimensional nanostructures, semiconductor nanowires (NWs) and quantum dots (QDs) have drawn more and more attention due to their unique characteristics. Semiconductor NWs have shown significant potential as building blocks for future nanophotonic and nanoelectronic devices, including lasers, photodetectors, light-emitting diodes (LEDs), and field-effect transistors (FETs).[1−4] While QD has been successfully applied to some planar optoelectronic devices, such as low threshold current QD lasers due to its strong confinement on electrons and photons.[5,6] A structure that combines the NWs with QDs is expected to have more functions and superior properties. In recent years, a hybrid structure fabricated by embedding a QD in a NW has been widely studied.[7−13] In contrast, another attractive structure that is fabricated by growing Stranski−Krastanow (S−K) QDs on the NW surface has been rarely reported.[14−17] Currently, studies on this structure still remain at an elementary level. Some deeper issues related to the structure, e.g., the variation of QDs with the deposition time as well as the relationship between the NW and QDs, have not been reported previously.

Up to now, the optical properties of InAs QDs on GaAs NWs have only been reported by Uccelli et al.[16] However, they only reported the photoluminescence (PL) emission at 4 K. The room temperature PL emission, which determines whether the structure can come into application to some extent, still needs to be studied further. Moreover, Qian et al. has reported a multiquantum-well NW heterostructure in which the gain medium was decoupled from the cavity.[1] They believed that a decoupling of the gain medium and cavity has more advantages compared with homogeneous nanowire systems.[18−20] The NW-QDs structure discussed in this work is expected to be another decoupling structure as the QDs and NW act as the gain medium and cavity, respectively.

In this paper, several samples of GaAs NW-InAs QDs structures were fabricated by Au-catalyzed metal organic chemical vapor deposition (MOCVD). The influence of the deposition time of InAs and the diameter of NWs on the formation of QDs was discussed. A model was proposed to describe the evolution process of QDs. The room temperature PL emission as well as the temperature dependence of the optical properties of InAs QDs was investigated. The resonance effect was also discussed.

The Au-assisted vapor−liquid−solid (VLS) growth was performed by using a Thomas Swan CCS-MOCVD system at a pressure of 100 Torr. Trimethylgallium (TMGa), trimethylindium (TMIn), and arsine were used as precursors. The carrier gas was hydrogen. Growth was carried out in the following steps: (1) An Au film with a thickness of 4 nm was deposited on GaAs (111)B substrate by magnetron sputtering; (2) the Au-coated GaAs substrate was loaded into the MOCVD reactor and annealed at 650 °C under arsine ambient for 300 s to form the Au−Ga alloyed particles as catalyst; (3) after being ramped down to the desired temperature, GaAs NWs were grown at 440 °C for 400s. TMGa was switched off after growth, while the flow rate of AsH_3 was kept constant at 2.87×10^{-3} mol min^{-1}; and (4) after raising the temperature to 475 °C, growth

Received: November 29, 2011
Revised: March 20, 2012
Published: March 22, 2012

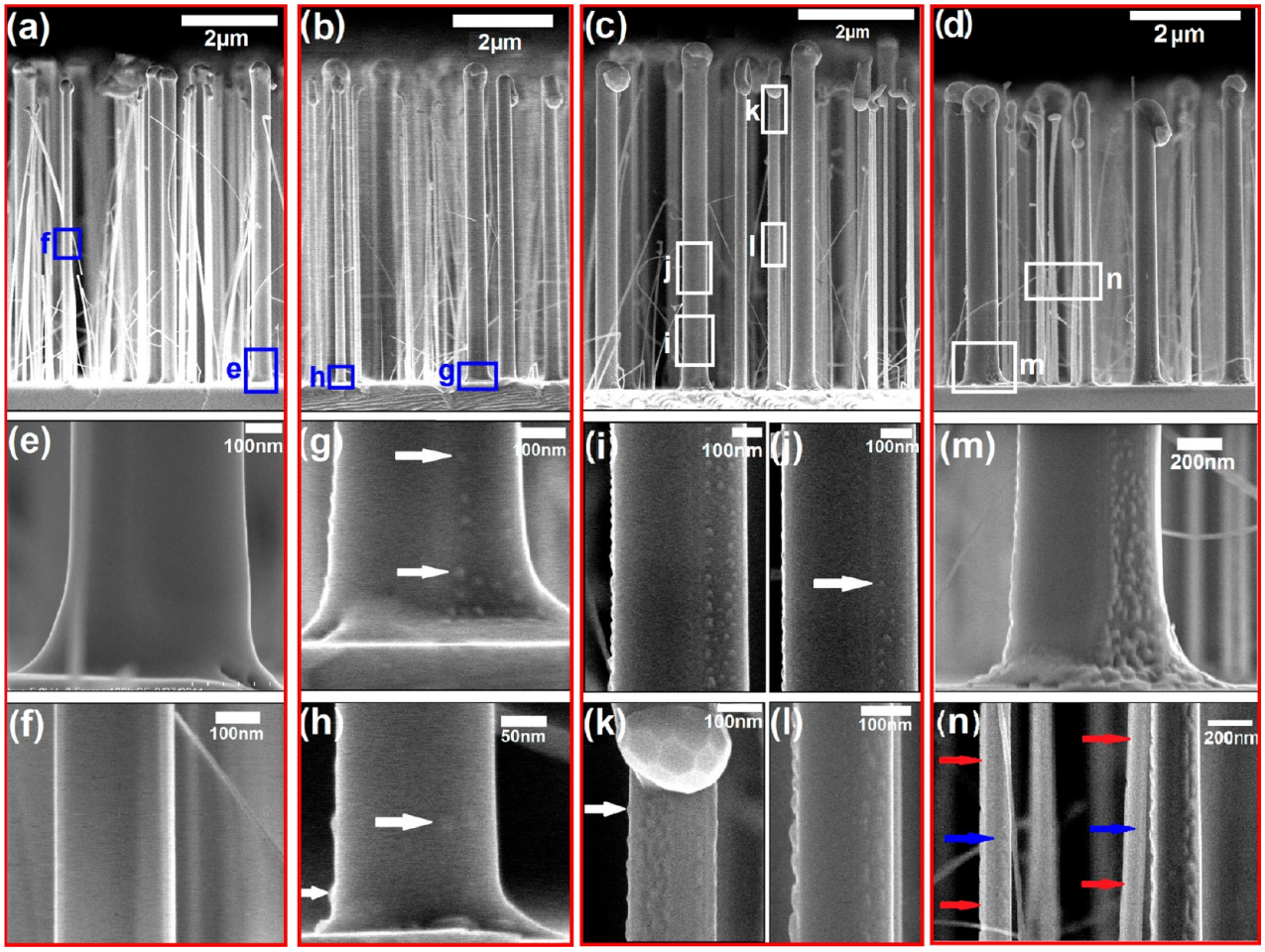

Figure 1. Cross sectional SEM images of samples 1−4: (a,e,f) correspond to sample 1; (b,g,h) correspond to sample 2; (c,i−l) correspond to sample 3; and (d,m,n) correspond to sample 4. Some of the QDs are indicated by white arrows. In (n), InAs shells formed by the coalescence of QDs are indicated by red arrows, while the GaAs cores are indicated by blue arrows.

of InAs was initiated with a TMIn flow rate of 11.3 μmol min^{-1} and an AsH_3 flow rate of 71.8 μmol min^{-1}.

To investigate the formation mechanism and evolution process of InAs QDs, four samples with different deposition time of InAs were fabricated. For samples 1, 2, 3, and 4, the deposition time of InAs was set to 30s, 50s, 70s, and 90s, respectively. To study the optical properties of these QDs, sample 5 was prepared by growing a thin GaAs shell after the InAs QDs in sample 3.

Morphologies of the samples were characterized by field emission scanning electron microscopy (FESEM). The structure and composition characteristics of the samples were investigated by transmission electron microscopy (TEM) and energy dispersive spectroscopy (EDS). TEM specimens were prepared by ultrasonicating the samples in ethanol for 5 min, followed by spreading drops from the suspension onto a holey carbon/Cu grid. For optical characterization, as-grown NWs were mechanically cut down and dispersed onto a SiO_2-coated Si substrate. The microphotoluminescence (μPL) measurements were carried out using a 632.8 nm continuous-wave He−Ne laser for excitation. The excitation beam was focused onto ~1 μm in diameter with a 50× microscope objective on the sample placed in a cryostat. The emission through the same microscope objective was collected into a liquid-N_2-cooled charge-coupled device (CCD) for spectral analysis.

Figure 1 shows the SEM images of samples 1−4. Nearly all the NWs in the four samples are vertical to the substrate, with diameters ranging from several dozens of nanometers to several hundreds and heights around 5−6 μm. Figure 1e,f shows the foot and middle parts of two single NWs (the diameter is 460 and 270 nm for the NW in (e,f), respectively) from sample 1, respectively. Both the lateral surfaces of the two NWs are smooth, without any QDs. Instead, EDS analyses demonstrate a very thin and even InAs shell outside the GaAs NW, as shown in Figure 2a. With the increasing of InAs deposition time, QDs begin to form, as shown in Figure 1g−n. This is very consistent with the S−K growth of QDs on a planar substrate that when the film (wetting layer) thickness exceeds some critical value, 3D QDs appear.[21] However, as the NW could share more strain energy caused by the lattice mismatch due to its unique characteristics, e.g., the large surface area/volume ratio and nanosized curve surface, the critical thickness of the "wetting shell" should be thicker than the wetting layer in the planar growth.[22,23]

Figure 1g,h shows the foot of two single NWs from sample 2, with a diameter of 400 and 177 nm, respectively. We can clearly find some QDs on both the surfaces. These QDs distribute very separately and disappear quickly at a distance about several hundreds of nanometers from the substrate. The formation of these QDs could be attributed to the adatom diffusion mechanism as well as the collection of Au particle on In

dx.doi.org/10.1021/nl204204f | Nano Lett. 2012, 12, 1851−1856

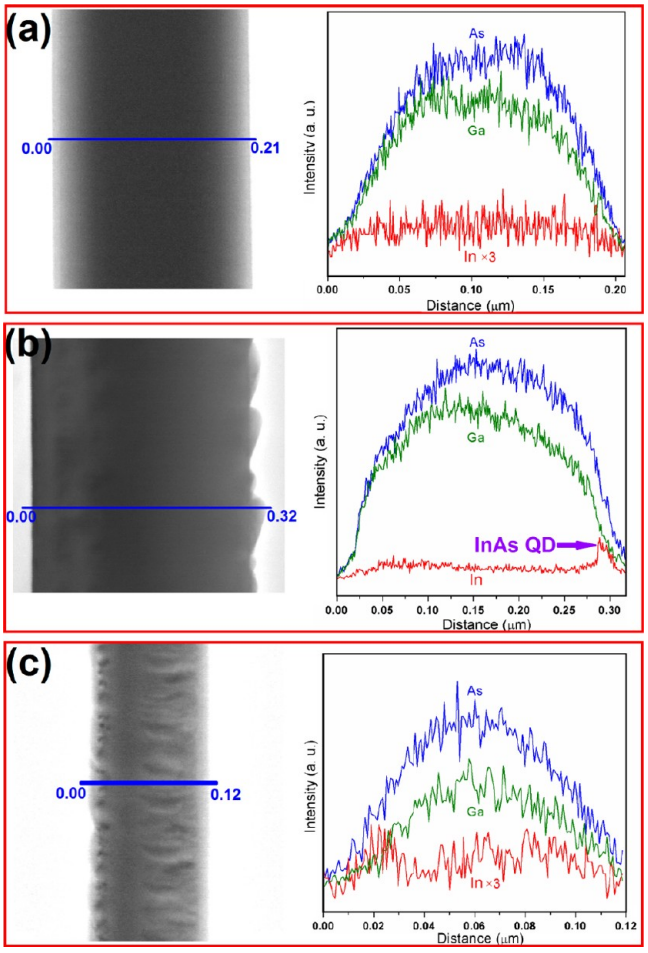

Figure 2. EDS analyses of NWs from (a) sample 1, (b) sample 3, and (c) sample 4.

adatoms, which has been reported in our previous work.[17] We also find that the QDs on the thinner NW are much sparser than those on the thicker one. According to research on thin film growth, as the substrate dimension is reduced, the thickness of the strained epitaxial film will increase since the strain energy is distributed more evenly between the epilayer and the substrate.[24] Thus the wetting shell of a thinner NW is expected to be thicker than a thicker NW. As a result, a thicker NW is easier to form QDs than a thinner one, as less In adatoms contribute to the formation of wetting shell while more contribute to the formation of QDs.

When the deposition time of InAs further increases, plenty of QDs are observed. Figure 1i,j corresponds to different parts of a single NW from sample 3 whose diameter is 430 nm. We can find that the QDs are very dense and aligned in several ribbons along the sidewalls of the NW at the lower part. Toward the top of the NW, QDs become sparser and disappear at a distance about 2.8 μm from the substrate. While for a much thinner one with a diameter of about 190 nm, the QDs have covered the whole NW surface from the bottom up as shown in Figure 1k,l. To investigate the relationship between the coverage range of the QDs and the diameter of the NW, we chose 30 NWs with different diameters and measured the length between the highest QD and the substrate. The results are shown in Figure 3. We can see that these values fall in three ranges. When the diameter is larger than 250 nm, all the NWs are partly covered with QDs. The coverage length of QDs

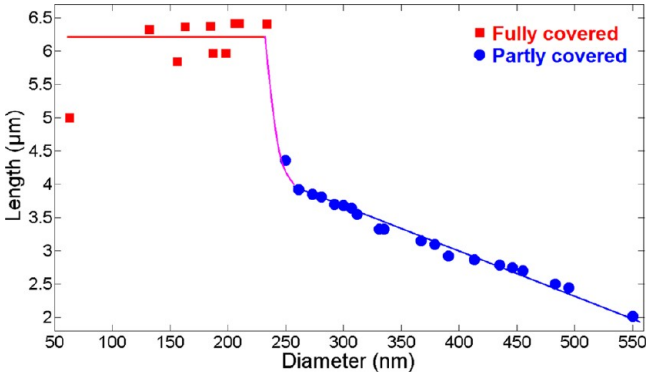

Figure 3. Relationship between the coverage length of the QDs and the diameter of the NWs for sample 3.

almost increases linearly with the decreasing of the diameter. When the diameter drops below 250 nm, the coverage length increases much more quickly and rapidly saturates at a diameter of 234 nm. When the diameter decreases further, all the NWs are fully covered with QDs from the bottom up. The fluctuation of coverage lengths in the fully covered range corresponds to the fluctuation of the heights of the as-grown GaAs NWs. In our previous work, we have demonstrated that these QDs are formed mainly by adatom diffusion from the substrate.[17] As the surface area per unit height of a thinner NW is smaller than that of a thicker one, less In adatoms are expected to be consumed per unit height. As a result, more In adatoms can diffuse to a higher position, and InAs QDs are formed. As mentioned before, the coverage length increases much more quickly when the diameter drops below 250 nm. It is possible that the NW could not form a sufficient amount of QDs as those thicker ones per unit area when the diameter is rather small. When the diameter further decreases, the NW is fully covered with QDs and coverage length saturates, which means that some of In adatoms diffusing beyond the NW height have been incorporated into the Au particle. Quantitative analysis about the relationship between the coverage length of QDs and the diameter of NWs, which probably involves growth kinetics, thermodynamics, and strain theory, will need to be studied further.

From Figure 3, we can determine that the critical diameter under which the NW can be fully covered by QDs is between 234 and 250 nm. Thus by adjusting the diameter of NWs, we can fabricate NW arrays with different coverage lengths of QDs for various applications.

When the deposition time was further lengthened to 90 s, the coalescence of QDs is observed. Figure 1n shows three single NWs from sample 4, with a diameter of 70, 120, and 210 nm, respectively. For the thickest one, we can see the QDs are closely aligned and have formed a discontinuous thin shell. While for the two thinner ones, a quasi-continuous thin InAs shell could be observed evidently outside the two cores. The EDS analyses of a single NW from sample 4 (Figure 2c) also demonstrate an InAs shell of about 20 nm outside the GaAs core. Compared with Figure 2b, we can clearly find the difference between a single QD and the coalescence of QDs.

Based on the discussions mentioned above, the evolution process of InAs QDs on the surface of GaAs NWs is clear. To illustrate the process, a simple model was proposed, as shown in Figure 4. Figure 4A shows the adatom diffusion mechanism which contributes to the formation of QDs. Figure 4B–D

dx.doi.org/10.1021/nl204204f | Nano Lett. 2012, 12, 1851–1856

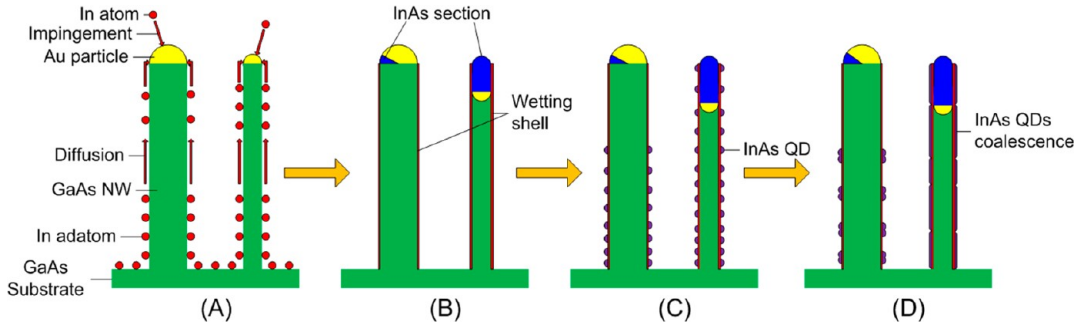

Figure 4. A schematic diagram of the evolution process of InAs QDs on the surface of GaAs NWs.

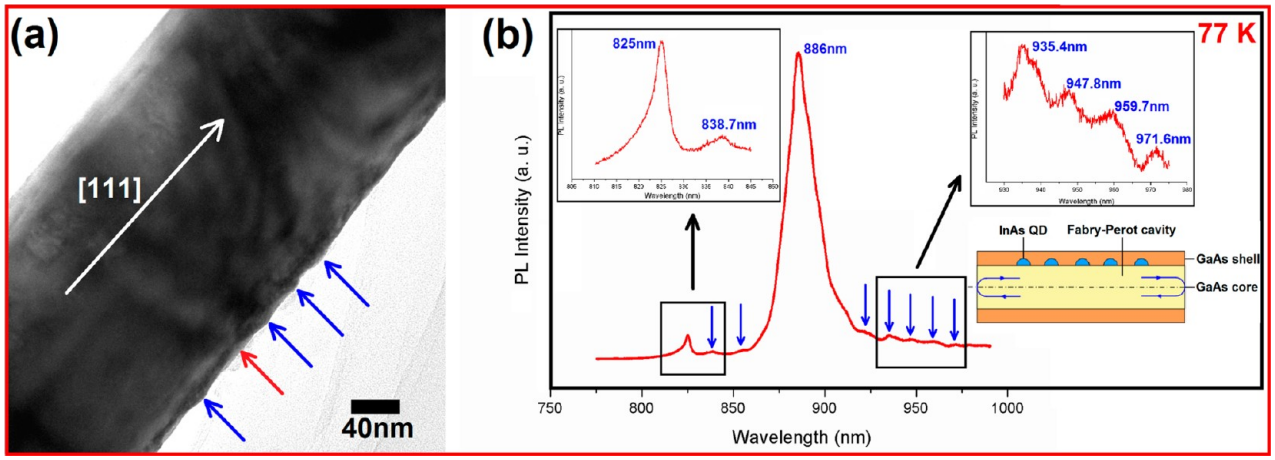

Figure 5. (a) TEM image of a single NW from sample D. The QDs buried by the GaAs shell are indicated by blue arrows. The red arrow indicates the GaAs shell between two QDs. (b) 77 K PL spectra of a single NW from sample D. The blue arrows show the resonant peaks. The insets show the GaAs peak and the resonant peaks as well as a schematic diagram of a Fabry–Perot cavity formed in the GaAs NW.

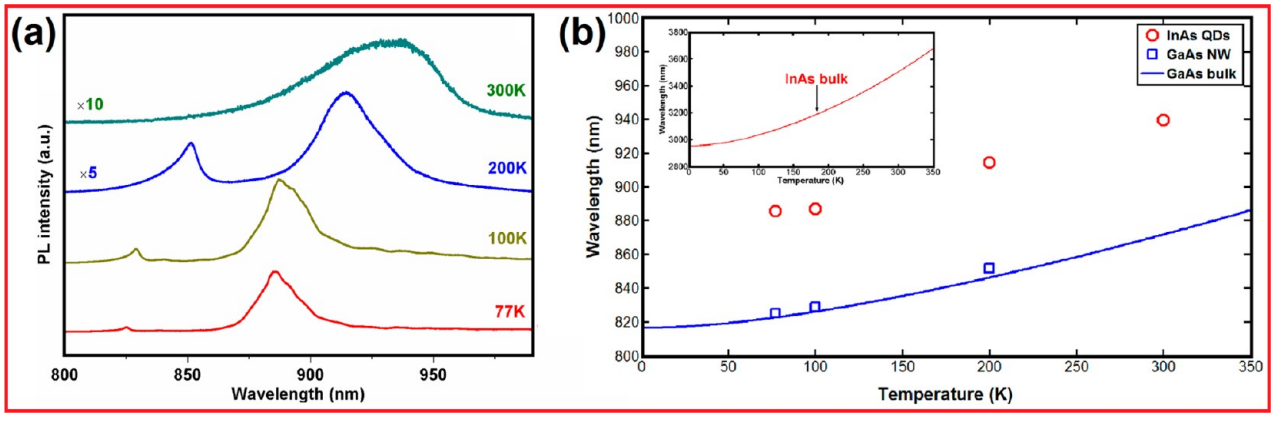

Figure 6. (a) Temperature-dependent PL spectral features from a single NW. (b) Plots of temperature-dependent PL wavelengths of the GaAs NW and InAs QDs. Theoretical temperature dependence on GaAs and InAs bandgaps (shown in the inset) is also given in the curve for comparison.

corresponds to the formation of wetting shell, formation of QDs, and the coalescence of QDs, respectively.

Now we turn to study the optical properties of this hybrid structure. Figure 5a shows the TEM image of a single NW from sample 5. We can clearly see that the QDs are buried by a thin shell. Figure 5b shows the corresponding PL spectra at 77 K. We can find two main peaks at 825 and 886 nm, respectively. The peak at 825 nm corresponds to the GaAs NW, as it is very close to the theoretical value (822.5 nm) of bulk GaAs at 77 K.[25] In addition, the line width of this peak is as narrow as 9.7 meV, which is comparable to line widths observed in high-purity GaAs NWs at 18 K (7 meV) and single InP NWs at 4 K (5.1 meV).[26,27] This indicates that these GaAs NWs are of high quality and high purity. However, the peak intensity is still very weak due to nonradiative recombination of photoexcited carriers at the sidewall surface where high density of surface states exists.[28] The other peak centered at 886 nm with a line width of 30 meV is attributed to the InAs QDs. We find that the intensity of this peak is much higher (up to 12 times higher) than the emission from the GaAs NW. In addition, a series of periodic peaks could be observed in PL spectra ranging from 838 to 972 nm with nearly the same wavelenth spacing (about 12 nm). These peaks probably correspond to the Fabry–Perot resonance peaks of the InAs QDs. It has been

dx.doi.org/10.1021/nl204204f | Nano Lett. 2012, 12, 1851–1856

proved that if the ends of the NW are smooth enough, they can function as two reflecting mirrors that define a Fabry–Perot cavity with modes $m(\lambda/2n) = L$, where m is an integer, λ is the wavelength, n is the refractive index, and L is the length of the cavity.[29,30] For Fabry–Perot cavity, the mode spacing $\Delta\lambda$ for a cavity with length L is given by $\Delta\lambda = \lambda^2/\{2L[n - \lambda(dn/d\lambda)]\}$, where $n - \lambda(dn/d\lambda)$ is the group refractive index. As reported by Hua et al., the group index is about 4.8 when the wavelength is 886 nm.[31] In our experiment, the length of the NW is estimated to be 6.5 μm. The theoretical value of the mode spacing $\Delta\lambda$ is calculated to be 12.6 nm, which is very close to our experimental result (12 nm). This demonstrates that the GaAs NW acts as a Fabry–Perot cavity, as schematically drawn in Figure 5b. Moreover, in this structure, InAs QDs act as a gain medium and produce light, while the GaAs NW functions as Fabry–Perot cavity, which means that the gain medium and the cavity are decoupled. Thus the laser wavelength output could be designed with independent optimization of the cavity, which is an obvious advantage compared with NW homogenious structures.

Figure 6a exhibits temperature-dependent PL spectra of a single NW from sample 5. The PL spectra were recorded at 77, 100, 200, and 300 K, respectively. As temperature increases, both the two main peaks exhibit a pronounced red shift and a broader line width. From Figure 6a we can see that the red shift of GaAs NW agrees very well with the temperature-dependent redshift of bulk GaAs. At room temperature, only the peak of the InAs QDs is observed, which is centered at about 940 nm with a line width of 86 meV. The wavelength is much shorter than that of the InAs QDs formed on GaAs (100) planar substrate,[31,32] which is probably due to the different surface characteristics between (112) and (100) as well as the different morphology of the QDs. The line width value is of the same order of magnitude as that on traditional GaAs (100) planar substrate, which indicates good optical properties of the QDs. However, the line width here is still a little larger than that on planar substrate (typically 40–60 meV),[31] which can be attributed to the size uniformity of these QDs.[33] Nevertheless, we think that the optical properties of the QDs could be further improved by using some special growth techniques, such as a low InAs growth rate and an InGaAs strain-reducing capping shell which have been used universally in the growth of QDs on planar substrate.[31,34]

In conclusion, we have successfully fabricated InAs QDs on the surface of GaAs NWs by Au-catalyzed MOCVD. We find that the deposition time of InAs has a considerable influence on the formation of InAs QDs. The diameter of GaAs NW can also affect the coverage length of InAs QDs. A model based on the adatom diffusion mechanism was proposed to describe the evolution process of InAs QDs on GaAs NWs. The emission from the InAs QDs was observed at room temperature, and the peak was centered at 940 nm with a line width of 86 meV. In addition, a series of resonant peaks can be observed at low temperature, which is attributed to the Fabry–Perot cavity formed in the GaAs NW. This hybrid structure shows great promise in the NW-based optoelectronic devices due to the excellent optical properties as well as the unique decoupling ability.

AUTHOR INFORMATION

Corresponding Author

*E-mail: xzhang@bupt.edu.cn; xmren@bupt.edu.cn

Notes

The authors declare no competing financial interest.

ACKNOWLEDGMENTS

This research was supported by the National Basic Research Program of China (2010CB327600), the National Natural Science Foundation of China (61020106007 and 61077049), New Century Excellent Talents in University (NCET-08-0736), and the 111 Program of China (B07005).

REFERENCES

(1) Qian, F.; Li, Y.; Gradečak, S.; Park, H.; Dong, Y.; Ding, Y.; Wang, Z.; Lieber, C. M. *Nat. Mater.* **2008**, *7*, 701.
(2) Pettersson, H.; Trägårdh, J.; Persson, A. I.; Landin, L.; Hessman, D.; Samuelson, L. *Nano Lett.* **2006**, *6*, 229.
(3) Qian, F.; Gradečak, S.; Li, Y.; Wen, C. Y.; Lieber, C. M. *Nano Lett.* **2005**, *5*, 2287.
(4) Xiang, J.; Lu, W.; Hu, Y.; Wu, Y.; Yan, H.; Lieber, C. M. *Nature* **2006**, *441*, 489.
(5) Klimov, V. I.; Mikhailovsky, A. A.; Xu, S.; Malko, A.; Hollingsworth, J. A.; Leatherdale, C. A.; Eisler, H. –J.; Bawendi, M. G. *Science* **2000**, *290*, 314.
(6) Badcock, T. J.; Royce, R. J.; Mowbray, D. J.; Skolnick, M. S.; Liu, H. Y.; Hopkinson, M.; Groom, K. M.; Jiang, Q. *Appl. Phys. Lett.* **2007**, *90*, 111102.
(7) Panev, N.; Persson, A. I.; Sköld, N.; Samuelson, L. *Appl. Phys. Lett.* **2003**, *11*, 2238.
(8) Borgström, M. T.; Zwiller, V.; Müller, E.; Imamoglu, A. *Nano Lett.* **2005**, *5*, 1439.
(9) Minot, E. D.; Kelkensberg, F.; Kouwen, M.; Dam, J. A.; Kouwenhoven, L. P.; Zwiller, V.; Borgström, M. T.; Wunnicke, O.; Verheijen, A. V.; Bakkers, E. P. A. M. *Nano Lett.* **2007**, *7*, 367.
(10) Tribu, A.; Sallen, G.; Aichele, T.; André; Poizat, J.; Bougerol, C.; Tatarenko, S.; Kheng, K. *Nano Lett.* **2008**, *8*, 4326.
(11) Singh, R.; Bester, G. *Phys. Rev. Lett.* **2009**, *103*, 063601.
(12) Claudon, J.; Bleuse, J.; Malik, N. S.; Bazin, M.; Jaffrennou, P.; Gregersen, N.; Sauvan, C.; Lalanne, P.; Gérard, J. M. *Nat. Photonics* **2010**, *4*, 174.
(13) Reimer, M. E.; Kouwen, M. P.; Barkelid, M.; Hocevar, M.; Weert, M. H. M.; Algra, R. E.; Bakkers, E. P. A. M.; Borgström, M. T.; Schmid, H.; Riel, H. *J. Nanophotonics* **2011**, *5*, 053502.
(14) Pan, L.; Lew, K.; Redwing, J. M.; Dickey, E. C. *Nano Lett.* **2005**, *5*, 1081.
(15) Ramlan, D. G.; May, S. J.; Zheng, J.; Allen, J. E.; Wessels, B. W.; Lauhon, L. J. *Nano Lett.* **2006**, *5*, 50.
(16) Uccelli, E.; Arbilo, J.; Morante, J. R.; Morral, A. F. *ACS Nano* **2010**, *4*, 5985.
(17) Yan, X.; Zhang, X.; Ren, X. M.; Huang, H.; Guo, J. W.; Guo, X.; Liu, M. J.; Wang, Q.; Cai, S. W.; Huang, Y. Q. *Nano Lett.* **2011**, *11*, 3941.
(18) Huang, M. H.; Mao, S.; Feick, H.; Yan, H.; Wu, Y.; Kind, H.; Weber, E.; Russo, R.; Yang, P. *Science* **2001**, *292*, 1897.
(19) Johnson, J. C.; Chol, H.; Knutsen, K. P.; Schaller, R. D.; Yang, P.; Saykally, R. J. *Nat. Mater.* **2002**, *1*, 106.
(20) Agarwal, R.; Barrelet, C. J.; Lieber, C. M. *Nano Lett.* **2005**, *5*, 917.
(21) Moison, J. M.; Houzay, F.; Barthe, F.; Leprince, L.; Andre, E.; Vatel, O. *Appl. Phys. Lett.* **1994**, *64*, 196.
(22) Wang, H.; Upmanyu, M.; Ciobanu, C. V. *Nano Lett.* **2008**, *8*, 4305.
(23) Li, X.; Yang, G. *J. Phys. Chem. C* **2009**, *113*, 12402.
(24) Lo, Y. H. *Appl. Phys. Lett.* **1991**, *58*, 2311.
(25) Levinshtein, M.; Rumyantsev, S.; Shur, M. World Scientific Press: Singapore, 1999; pp 65–66.
(26) Joyce, H. J.; Gao, Q.; Tan, H. H.; Jagadish, C.; Kim, Y.; Fickenscher, M. A.; Perera, S.; Hoang, T. B.; Smith, L. M.; Jackson, H. E.; Yarrison-Rice, J. M.; Zhang, X.; Zou, J. *Adv. Funct. Mater.* **2008**, *18*, 3794.

(27) Chuang, L. C.; Moewe, M.; Chase, C.; Kobayashi, N. P.; Chang-Hasnain, C. *Appl. Phys. Lett.* **2007**, *90*, 043115.
(28) Noborisaka, J.; Motohisa, J.; Hara, S.; Fukui, T. *Appl. Phys. Lett.* **2005**, *87*, 093109.
(29) Duan, X. F.; Huang, Y.; Agarwal, R.; Lieber., C. M. *Nature* **2003**, *421*, 241.
(30) Hua, B.; Motohisa, J.; Ding, Y.; Hara, S.; Fukui, T. *Appl. Phys. Lett.* **2007**, *91*, 131112.
(31) Nishi, K.; Saito, H.; Sugou, S.; Lee, J. S. *Appl. Phys. Lett.* **1999**, *74*, 1111.
(32) Ru, E. C. L.; Howe, P.; Jones, T. S.; Murray, R. *Phys. Rev. B* **2003**, *67*, 165303.
(33) Leon, R.; Fafard, S.; Leonard, D.; Merz, J. L.; Petroff, P. M. *Appl. Phys. Lett.* **1995**, *67*, 115175.
(34) Ray, M.; David, C.; Surama, M.; Philip, S.; Christine, R.; Michel, H. J.; Paul, S. *Jpn. J. Appl. Phys.* **1999**, *38*, 528.